View metadata, citation and similar papers at core.ac.uk

brought to you by CORE

provided by Institutional Research Information System University of Turin

Magnetic power losses in $[(Fe_{1-x}Co_x)_{75}B_{20}Si_5]_{93}Nb_4Y_3$ (x = 0, 0.2, 0.4) bulk metallic glasses

This content has been downloaded from IOPscience. Please scroll down to see the full text.

2009 J. Phys.: Conf. Ser. 144 012073

(http://iopscience.iop.org/1742-6596/144/1/012073)

View the table of contents for this issue, or go to the journal homepage for more

Download details:

IP Address: 95.74.72.137

This content was downloaded on 26/04/2014 at 18:55

Please note that terms and conditions apply.

Magnetic Power Losses in $[(Fe_{1-x}Co_x)_{75}B_{20}Si_5]_{93}Nb_4Y_3$ (x = 0, 0.2, 0.4) Bulk Metallic Glasses

R Piccin[1], P Tiberto[2], H Chiriac[3], M Baricco[1]

[1] Dipartimento di Chimica IFM and NIS, Università di Torino, Via P.Giuria 9, 10125 Torino, Italy

[2] Istituto Nazionale di Ricerca Metrologica INRIM, Strada delle Cacce 91, 10135 Torino, Italy

[3] National Institute of Research and Development for Technical Physics, 47 Mangeron Blvd, Iasi 700050, Romania

E-mail: rafael.piccin@unito.it

Abstract. Magnetic power losses of $[(Fe_{1-x}Co_x)_{75}B_{20}Si_5]_{93}Nb_4Y_3$ (x = 0, 0.2, 0.4) metallic glasses have been investigated. Bulk samples were prepared by water-cooled Cu-mold injection casting technique with shapes of cylinders (0.8 mm diameter and 30 mm length) and toroids (10 mm external diameter and 0.5 mm thickness). Ribbons prepared by the melt-spinning technique were also analyzed. Glassy structures were confirmed by the presence of a main halo in XRD and by crystallization signal in DSC. Power losses were studied with a digital wattmeter over a range of frequencies from 1 to 400 Hz at selected peak inductions. Ribbons show smaller losses than bulk samples, presenting 24.5 J/m^3 at 50 Hz and 0.65 T peak induction. It was observed that the Co addition reduces significantly the power losses. A separation theory was applied in order to explain the square root behavior of the measured power losses as a function of frequency and the results are in good agreement with the experimental data. The magnetic data were used to identify the presence of crystalline inclusions in the magnetic bulk metallic glasses. The effect of sample shape and composition on magnetic properties will be discussed.

1. Introduction

Fe-based amorphous alloys have drawn considerable attention mainly due to their good soft magnetic properties, such as high saturation magnetization, low core loss, and high permeability [1]. The main fields of applications of such material are linked to the electrical industry and to the development of magnetic sensors. However, most of the Fe-based amorphous alloys present limited glass forming ability (GFA). In order to extend their application field much research efforts have been made to develop thicker amorphous magnetic materials. New multicomponent alloys have shown to have larger GFA, allowing direct cast from the liquid in a fully amorphous state at cooling rates around 10-100 K/s. Such characteristic allows preparation of objects of different shapes/geometry, extending the application fields. Nevertheless, soft magnetic properties of bulk metallic glasses are not optimized yet and continuing efforts to improve them have been made by modifying alloys composition and improving casting techniques [2]. In this purpose, we examined the effect of the different geometries

© 2009 IOP Publishing Ltd

with special emphasis on magnetic characterization and power losses on $[(Fe_{1-x}Co_x)_{75}B_{20}Si_5]_{93}Nb_4Y_3$ (x = 0, 0.2, 0.4) glassy alloys [3]. In particular, cylinders were examined in a closed configuration to rule out demagnetizing effects when comparing cylinders and toroids data. In this paper, diffraction measurements, magnetic properties and power losses of $[(Fe_{1-x}Co_x)_{75}B_{20}Si_5]_{93}Nb_4Y_3$ (x = 0, 0.2 and 0.4) cylindrical and toroidal bulk glassy alloys are presented and compared with that of as-cast ribbons with the same compositions.

2. Experimental

$[(Fe_{1-x}Co_x)_{75}B_{20}Si_5]_{93}Nb_4Y_3$ master alloys with x = 0, 0.2 and 0.4 (at.%) were prepared by melting appropriate amounts of pure elements in an arc furnace under Ti-gettered argon atmosphere. Melting was repeated several times in order to assure homogenization. Total weight loss due to arc-melting was less than 0.2 %. Cylindrical samples with diameter of 0.8 mm and toroidal samples with thickness of 0.5 mm, external and internal diameter of 10 mm and 6 mm, respectively, were prepared by water-cooled Cu-mold injection casting technique. Ribbons with thickness of 30 μm and width of 2 mm were prepared using the melt-spinning method. The structure of the as-cast samples was verified by X-ray diffraction (XRD) with Co Kα radiation (λ = 0.1789 nm). The microstructure of the samples was examined by scanning electron microscopy (SEM). Hysteresis loops were measured by a digital feedback wattmeter under sinusoidal induction waveform [4] in the frequency range from 1 to 400 Hz at selected peak induction. Power losses were obtained integrating the measured hysteresis loops. Feedback control was based on a computer-driven iterative procedure and was used to obtain a sinusoidal induction waveform B. Ribbon pieces 10 cm long were cut from a master piece to minimize demagnetizing effects. In order to avoid the strong demagnetizing effect in the bulk cylinders, a MnZn N30 ferrite frame (μ_i = 5000) [5] was used to close the magnetic flux and vanish the demagnetizing field.

3. Results and discussion

The XRD patterns of as-cast toroid, cylinders and ribbons are shown in figure 1. Results show the typical halo of a fully amorphous phase for all the analyzed compositions in all the studied shapes. These results emphasize that the GFA of $[Fe_{75}B_{20}Si_5]_{93}Nb_4Y_3$ alloy exhibits a good tolerance of Co addition, in agreement with our previous results for cylinders and ribbons [3].

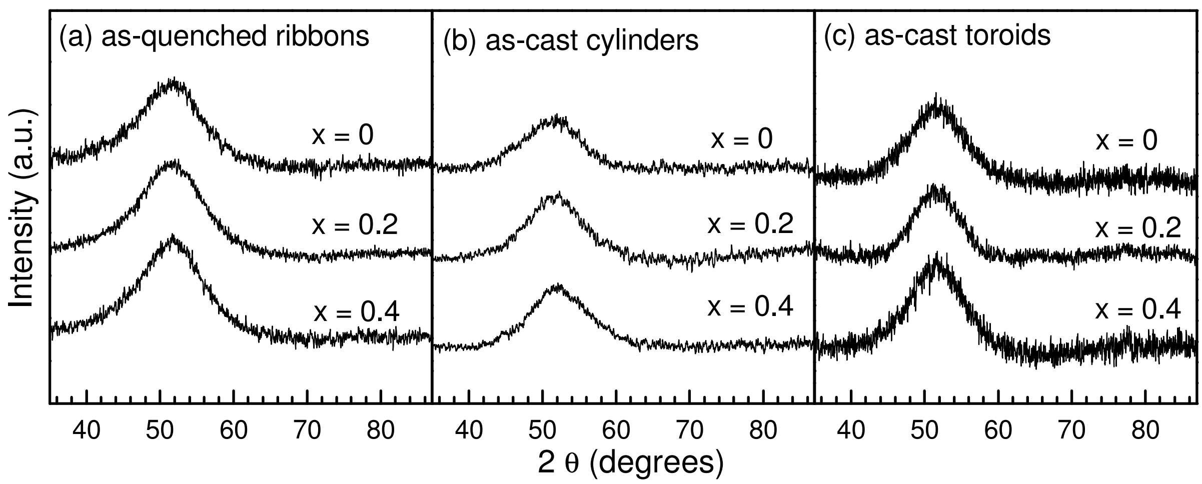

Figure 1. XRD patterns for as-cast $[(Fe_{1-x}Co_x)_{75}B_{20}Si_5]_{93}Nb_4Y_3$ (x = 0, 0.2 and 0.4) samples. (a) ribbons, (b) cylinders and (c) toroids.

Hysteresis loops were measured for all samples. Figure 2 shows hysteresis loops of amorphous ribbons, cylinders, closed cylinders and toroids of $[(Fe_{0.6}Co_{0.4})_{75}B_{20}Si_5]_{93}Nb_4Y_3$ alloy. Measurements were performed at 10 Hz with a fixed polarization of 0.65 T. From the shape of hysteresis loops, it appears that very different magnetization processes are observed due to the influence the demagnetizing field. The ribbon is easily magnetized due to its long aspect ratio, showing the highest initial permeability (μ_i) equal to 1624. In the case of the cylinder, the occurrence of a very strong demagnetizing field limits its μ_i to 323. Using the N30 ferrite frame, the magnetization process approaches the same behavior observed for the ribbon, showing $\mu_i = 1455$. In the case of the toroid, due to its closed shape, one would expect a result close to the ribbon. However, μ_i is only 270 due the presence of macroscopic surface defects produced during the casting. Such defects contribute to local stray fields that generate demagnetizing effects. Moreover, approaching the maximum field, the magnetization process is dominated by rotations that can be associated to the presence of defects inside the material, like pores or internal tensions.

Coercivity fields (H_C) for different sample geometry and for different composition are reported in table 1. In order to minimize dynamic contributions, H_C was determined extrapolating H_C against frequency to zero. Same H_C have been observed for opened and closed cylinder for all compositions since demagnetizing factor does not interfere in such a quantity. A slightly variation in H_C is observed in the case of ribbons when Co in added. However, a significant change is observed in the case of the as-cast cylinders, since for $x = 0.2$ and 0.4 H_C is lowered from 52 A/m to 2.0 and 3.9, respectively. Co addition was less effective in the case of amorphous toroids, lowering H_C from 7.0 to 6.6 A/m.

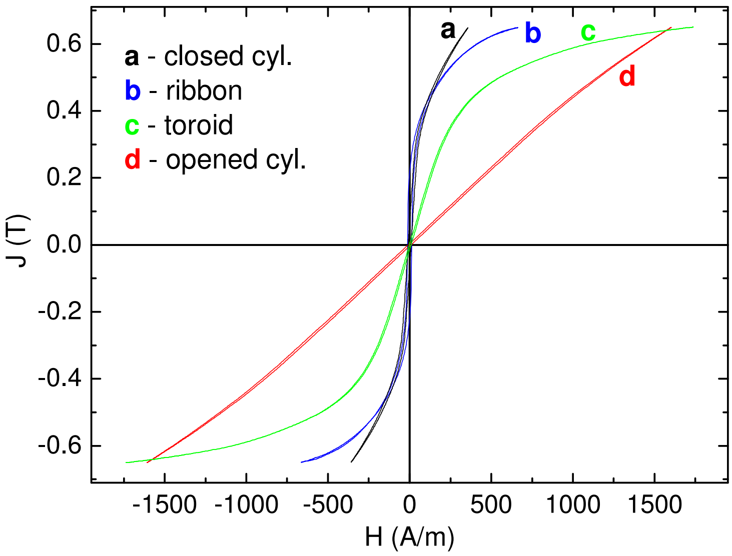

Figure 2. Hysteresis loops measured at a fixed polarization $J_p = 0.65$ T for $[(Fe_{0.6}Co_{0.4})_{75}B_{20}Si_5]_{93}Nb_4Y_3$ samples.

Table 1. H_C in $[(Fe_{1-x}Co_x)_{75}B_{20}Si_5]_{93}Nb_4Y_3$ (x = 0, 0.2 and 0.4) samples.

sample, x	0	0.2	0.4
Ribbon	2.0	3.2	4.7
Opened cylinder	52	2.0	3.9
Closed cylinder	52	2.0	3.9
Toroid	7.0	-	6.6

Figure 3 shows the results of power loss measurements performed in the frequency range from 1 to 400 Hz for $[(Fe_{0.6}Co_{0.4})_{75}B_{20}Si_5]_{93}Nb_4Y_3$ ribbon, opened cylinder, closed cylinder and toroid at fixed induction ($J_p = 0.65$ T). The toroid presents the lowest losses for frequencies below 100 Hz. Above such frequency, the ribbon exhibits the smallest power losses since its thickness makes the classical loss contribution much smaller. In the case of the cylinder, measurement performed with and without the closing frame give the same results indicating that in the studied frequency range the effect of demagnetizing field is limited. However, at 400 Hz, the skin effect associated with the smaller permeability of the opened cylinder leads to smaller losses. It's worth mentioning that toroid and cylinders samples show a strong increase in magnetic power losses above 100 Hz due to their bulky nature, that allows the formations of eddy currents, since the classical loss term depends on the square of the thickness [3,6].

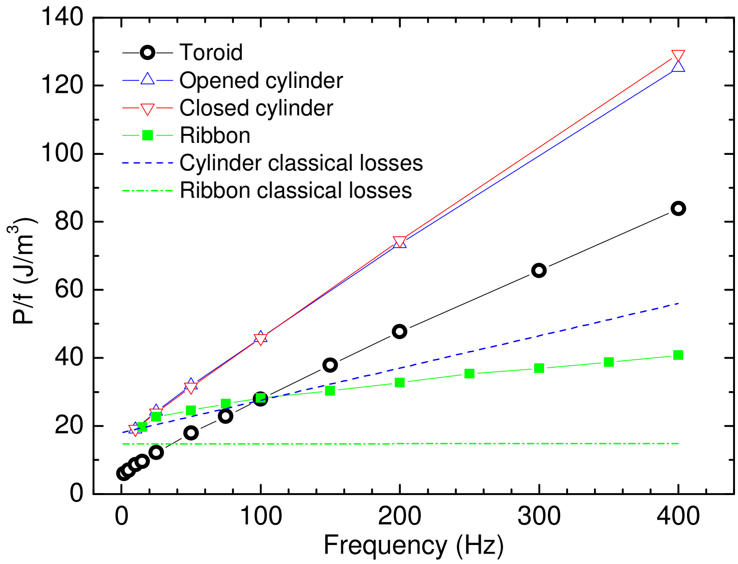

Figure 3. Magnetic power losses per cycle as functions of frequency for $[(Fe_{0.6}Co_{0.4})_{75}B_{20}Si_5]_{93}Nb_4Y_3$ samples at B_p = 0.65 T. Ribbons, cylinders, cylinder inside frame and toroids.

4. Conclusions

The addition of Co to $[Fe_{75}B_{20}Si_5]_{93}Nb_4Y_3$ amorphous alloys improved coercivity and power losses, without detrimental effects on the GFA. However, it is worth mentioning that demagnetizing effects and geometry defects can interfere on the properties related to technological applications, like the initial permeability. Moreover, it was shown that amorphous toroids can be developed showing power losses smaller than amorphous ribbons. However, this advantage is limited to very low frequencies, allowing their use in specific applications, like in static motor components, actuators and transformer cores. Conversely, such limitation rules out applications at high frequencies, like magnetic field sensors, due to strong classical losses associated with their bulky nature.

From the present results, it worth mentioning that the comparison between the magnetic properties of commercial ribbons, such as Metglas, Finemet and Nanoperm, and ribbons made from alloys optimized for production of bulk metallic glasses leads to awkward results, since the search for improving GFA does not necessarily leads to an improvement in the magnetic properties. However, good glass formers allows one to cast small devices close to its final geometry by near net shaping techniques, reducing costs and avoiding rolling processes that can change drastically magnetic properties and require further treatments to reestablish the initial properties.

Acknowledgements

This work is supported by Regione Piemonte and by Bilateral Italy-Romania Project n° 13. Dr. F. Fiorillo (INRIM) is acknowledged for fruitful discussions.

References

[1] McHenry M E, Willard M A, Laughlin D E 1999 *Prog. Mater. Sci.* **44** 291-433
[2] Shen B, Akiba M, Inoue A 2006 Phys. Rev. B **73** 104204
[3] Piccin R, Tiberto P, Chiriac H, Baricco M 2008 *J. Magn. Magn. Mater.* **320** e806-e809
[4] Bertotti G, Ferrara E, Fiorillo F, Pasquale M 1993 *J. Appl. Phys.* **73** 5375
[5] Beatrice C, Banu N, Ferrara E, Fiorillo F 2008 *J. Magn. Magn. Mater.* **320** e810-e813
[6] Bozorth R 1951 *Ferromagnetism* (Princeton, New Jersey: D. Van Nostrand Company)